Transactions, SMiRT-24
BEXCO, Busan, Korea - August 20-25, 2017
Division I

J-R FRACTURE TOUGHNESS OF COLD-WORKED TP316L STAINLESS STEEL UNDER SEISMIC LOADING CONDITIONS

Jin-Weon Kim[1], Myung-Rak Choi[2]

[1] Professor, Nuclear Engineering, Chosun University, Korea
[2] Graduate Student, Nuclear Engineering, Chosun University, Korea

ABSTRACT

This study conducted *J-R* fracture toughness test on as-received and 33% cold-worked stainless steel (SS) under dynamic and cyclic loading conditions to investigate the effect of seismic loading on the fracture behaviour of irradiated austenitic SSs. Cold-work is known to be a useful method to simulate irradiation embrittlement of structural materials, unless irradiation dose is less than a threshold level to nucleate voids and He-bobbles. The 33% cold-work is expected to simulate the mechanical properties of SSs irradiated up to approximately 15dpa. The *J-R* fracture toughness tests were carried out under monotonic load with quasi-static and dynamic loading rates and cyclic load with quasi-static loading rate at RT and 316^{o}C. The results showed that the fracture resistance of TP316L SS was considerably reduced by 33% cold-work, in particular the reduction was significant at 316^{o}C. The dynamic loading effect on fracture resistance was negligible for cold-worked TP316L SS regardless of test temperature. Cyclic load considerably reduced the fracture resistance of as-received TP316L SS, but the reduction by cyclic load was less significant for cold-worked TP316L SS compared to as-received TP316L SS. In particular, the cyclic loading effect was nearly diminished at 316^{o}C. This is because the fracture resistance of cold-worked TP316L SS is low enough so that the crack sharpening effect induced by cyclic load is insignificant.

INTRODUCTION

Interest in the integrity of systems, structures, and components (SSCs) of nuclear power plants (NPPs) under beyond design basis earthquake (BDBE) as well as design basis earthquake (DBE) conditions has greatly increased after the nuclear accident in the Fukushima Daiichi NPPs (Saji (2014)), and the integrity assessments of SSCs under excessive seismic loading are now required not only for newly designed NPPs but also for long-term operated NPPs (Saji (2014), Stevenson (2014)). Thus, reliable integrity assessment under excessive seismic loading conditions has become an important issue.

Since the SSCs of NPPs could plastically behave under excessive seismic loading conditions, the elastic-plastic behavior should be included in the integrity assessment and the mechanical properties, including the seismic loading characteristics such as dynamic and cyclic, should be considered in the integrity assessment. In this regard, a number of experimental studies carried out the cyclic stress–strain tests and characterized cyclic deformation and hardening/softening behaviors of structural materials for SSCs of NPPs (Nakamura et al.(2015), Paul et al. (2011), Goyal et al.(2013)). In addition, the fracture toughness tests have been conducted under dynamic and cyclic loading conditions and the fracture behavior of materials was evaluated under seismic loading conditions (Singh et al.(2003), Chowdhury et al.(2015), Roy et al.(2009), USNRC (1996), Kim et al. (2016)). It was reported that the fracture resistance of materials was significantly reduced by reversible cyclic loads versus that under monotonic load, and that the reduction depended on the load-history parameters such as compressive load level and frequency of the cyclic load. Also, it has been seen that the loading rate effect on the mechanical properties was negligible for austenitic stainless steels but the effect was considerable for ferrtitic steels (USNRC (1996), Kim et al. (2016)).

However, none of these investigations has taken into account age-related material degradation, although the materials of SSCs in long-term operated NPPs are degraded by long-term exposure to high temperature and corrosive and radiation environments. According to the studies on aging management of NPPs (Shah et al.(1993), Delliou et al.(2015)), the mechanical properties of materials change considerably with age-related degradation. To ensure the reliability of integrity assessments for SSCs in long-term operated NPPs under an excessive seismic loading condition, it is important to clarify the effects of seismic loading characteristics on the deformation and fracture behaviors of materials aged in the environment of NPPs. Therefore, this study conducted *J-R* fracture toughness tests on cold-worked TP316L stainless steel (SS), which simulates irradiation embrittlement, under dynamic and cyclic loading conditions at room temperature (RT) and the operating temperature of NPPs (316°C). Tensile tests were also carried out to obtain the reference mechanical properties for both materials under quasi-static and dynamic loading conditions. From the results of these tests, the effect of seismic loading characteristics on the fracture behavior of cold-worked TP316L austenite stainless steel was investigated.

EXPERIMENT

Test Material and Specimens

As-received and 33% cold-worked TP316L SSs were used for the experiment. TP316L SS is commonly used as structural material in the NPPs, especially it is used for reactor internal material. The previous studies showed that the cold-work can simulate the increase in strength and decrease in ductility and toughness of austenite SS by neutron irradiation, even though it cannot simulate the grain boundary segregation of impurities and generation of He-bubble (Jitsukawa et al.(1996)). Thus, this study used 33% cold-worked TP316L SS, which was expected to show the change in mechanical properties of SS irradiated up to approximately 15dpa (Pawel et al. (1996)).
J-R fracture toughness tests were performed using a compact tension (CT) specimen (thickness: 12.7 mm; width: 25.4 mm), which was designed in accordance with the ASTM E1820-15 standard (ASTM (2015)). All specimens were pre-cracked to a crack length (a_o) of 0.59 W, where W is the width of the specimen, and side-grooved on both sides of the specimen following the ASTM E1820-15 standard. A round-bar-type specimen (diameter: 5.0 mm; gage length: 25.0 mm), designed in accordance with the ASTM E8/E8M-09 standard (ASTM (2009)), was used for the tensile test. Figure 1 illustrates the CT specimen and tensile specimen used for experiment.

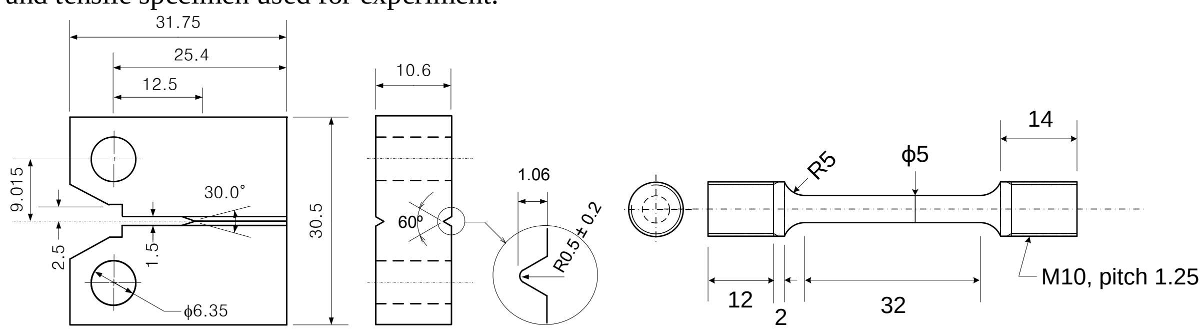

(a) 0.5T- CT specimen (b) Tensile specimen

Fig. 1 Specimens used for J-R fracture toughness and tensile tests

Experimental Procedure

J-R fracture toughness tests were conducted on both as-received and cold-worked TP316L SSs under monotonic and cyclic loading conditions at RT and 316°C. In case of monotonic tests, two different displacement rates (V_{LL}) were considered: V_{LL} = 0.45 and 1,140 mm/min. The cyclic *J-R* tests were conducted at V_{LL} = 0.45 mm/min. The displacement rate of 0.45 mm/min corresponds to a quasi-static loading rate, and V_{LL} = 1,140 mm/min corresponds to a typical dynamic loading rate. In general, a loading rate under seismic condition is considered to be 1,000–10,000 times faster than that typically used for quasi-static *J–R* fracture tests (ASTM (2015)). Thus, the displacement rate of 1,140 mm/min is believed to be a seismic loading rate.

For monotonic *J–R* tests, tensile displacement was applied monotonically to the specimen without unloading. For cyclic *J–R* tests, an incremental displacement-controlled cyclic load was applied following the loading sequence shown in Fig. 2. In the cyclic loading sequence, the displacement was controlled during the tensile loading step, while the load was controlled during the compressive loading step to maintain a constant cyclic load ratio ($R = P_{min}/P_{max}$). In the tests, the constant displacement increment (*d*) of 0.15 mm was applied after each cycle and the cyclic load ratio of $R = -1.0$ was used.

In the monotonic *J–R* tests, crack extension was determined by the normalization method defined in the ASTM E1820-15 standard, and the *J*-integral was calculated in accordance with the standard procedure. Crack extension in the cyclic tests was determined by a direct-current potential drop (d-c PD) method. Unlike the monotonic *J–R* test, no standard procedure for calculating *J*-integral under a cyclic loading condition is available. In the present study, the *J*-integral was calculated from the envelope area under the load versus load-line displacement (*LLD*) curve and above zero load, ignoring the compressive loading portion, in accordance with the ASTM standard procedure (ASTM (2015)). Figure 3 shows a sample of load versus *LLD* curve. The detailed procedure can be seen in our previous study (Kim et al.(2016)).

Tensile tests were also conducted on as-received and cold-worked TP316L SSs at RT and 316°C under quasi-static and dynamic strain rates: *i.e.*, $\dot{\varepsilon} = 5.21 \times 10^{-4}$ and $1.188\, s^{-1}$.

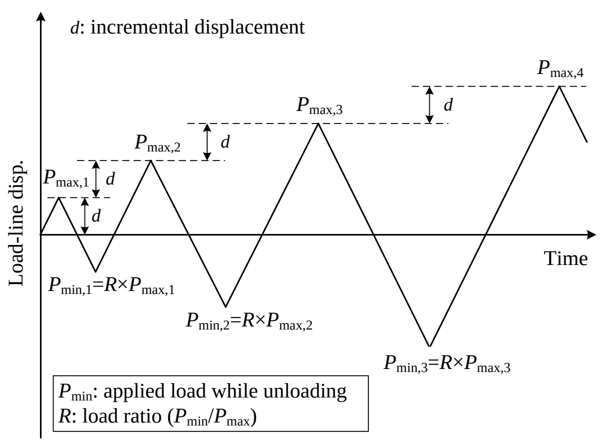

Fig. 2 Loading sequence applied to cyclic J-R fracture toughness test

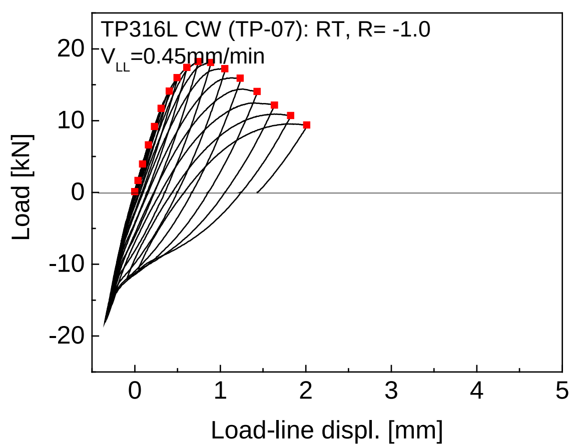

Fig. 3 A sample data obtained from cyclic J-R test

RESULTS AND DISCUSSION

Tensile Tests

Prior to *J-R* fracture toughness tests, tensile tests were conducted to obtain reference tensile properties of as-received and cold-worked TP316L SSs under quasi-static and dynamic displacement rates. Figure 4 presents the engineering stress-strain curves of as-received and cold-worked TP316L SSs tested at RT and 316°C under quasi-static displacement rate. In Fig. 4, regardless of test temperature, cold-worked TP316L SS that simulates irradiation embrittlement shows much higher strength and smaller elongation compared to as-received TP316L SS. For cold-worked TP316L SS, also, necking occurs immediately after elastic deformation without uniform deformation. The necking deformation is more significant at 316°C than at RT. Such deformation behaviours are also observed from the results of dynamic tensile tests. Compared with the results of tensile test on irradiated TP316 SS, it is indicated that these deformation behaviours of

cold-worked TP316L SS are consistent with those of irradiated material (Kim et al. (2010)). Thus, it is believed that the cold-work can properly simulate the tensile properties of irradiated TP316L SS.
Figure 5 compares the engineering stress-strain curves of cold-worked TP316L SS for different strain rates at RT and 316°C to investigate the dynamic loading effect on deformation of cold-worked TP316L SS. As shown in Fig. 5, at RT the strength increased and the ductility decreases as the displacement rate increases, while the effect of displacement rate on deformation behaviour of cold-worked TP316L SS is negligible at 316°C. This displacement rate dependency of cold-worked TP316L SS was nearly the same as that of as-received TP316L SS. Thus, it is indicated that the dynamic loading effect on stress-strain behaviour of TP316L SS is not altered by cold-work, even though the stress-strain behaviour is considerably changed by cold-work. Also, it can be expected from this result that the dynamic loading effect on deformation behaviour of irradiated TP316L SS is insignificant.

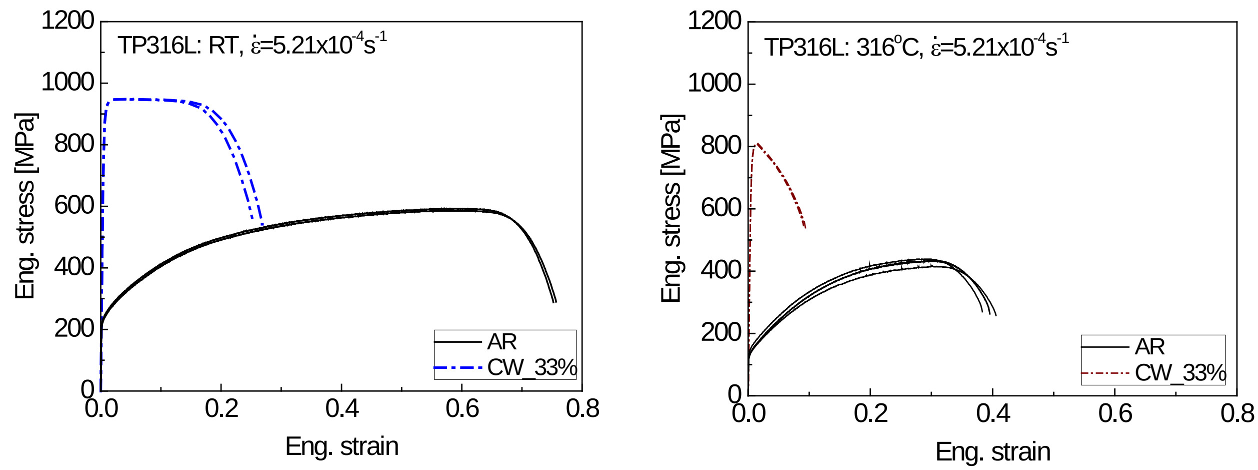

(a) RT (b) 316°C

Fig. 4 Comparison of engineering stress-strain curves of as-received and cold-worked TP316L SSs

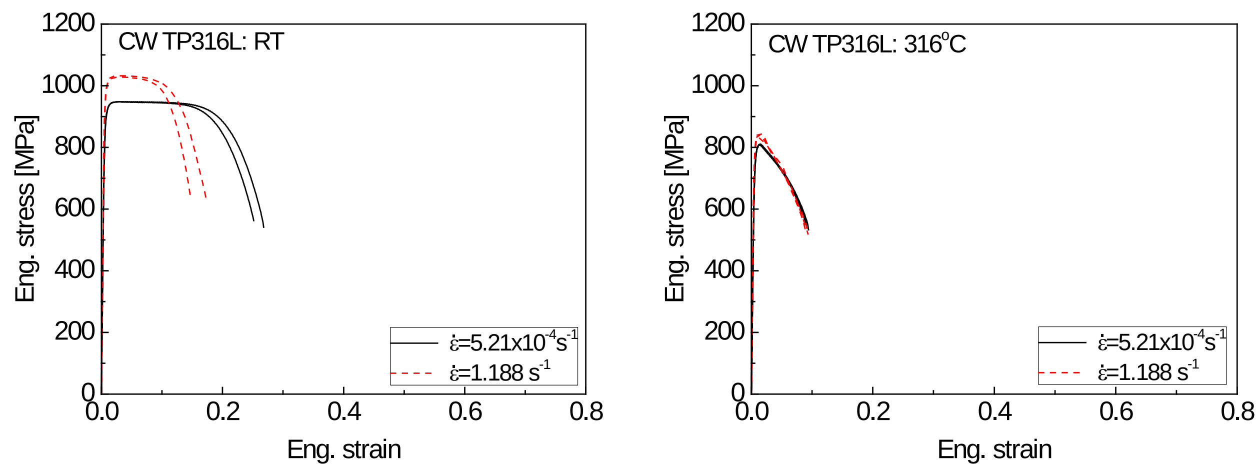

(a) RT (b) 316°C

Fig. 5 Comparison of engineering stress-strain curves of cold-worked TP316L SSs at different strain rates

***J-R* Toughness Tests**

Figure 6 presents monotonic *J-R* curves of as-received and cold-worked TP316L SSs tested at RT and 316°C under quasi-static displacement rate (V_{LL}=0.45mm/min). As shown in Fig. 6, the *J-R* curves of cold-worked TP316L SS are much lower than those of as-received TP316L SS; i.e., the fracture resistance of TP316L SS is considerably reduced by 33% cold-work. In particular, the reduction in *J-R* curves is significant at 316°C; the reduction rate is about 85%. This effect of cold-work on fracture resistance is also observed under dynamic displacement rate. Comparison of load versus *LLD* curves of as-received and cold-worked TP316L SSs shows that the cold-work considerably increases maximum load and decreases displacement to maximum load of TP316L SS. This indicates that the significant reduction in fracture resistance of cold-worked TP316L SS is mainly attributed to reduction in ductility by cold-work. Also, the present results confirm that the cold-work appropriately simulates the irradiation embrittlement of TP316L SS as reported by previous study (Jitsukawa et al.(1996)).

Figure 7 compares the quasi-static and dynamic *J-R* curves of cold-worked TP316L SS at RT and 316°C to investigate the effect of loading rate on fracture resistance of cold-worked TP316L SS simulating irradiation embrittlement. As shown in Fig. 7, regardless of test temperature, the *J-R* curves of cold-worked TP316L SS at both quasi-static and dynamic are almost identical; i.e., the fracture toughness of cold-worked TP316L SS is independent of loading rate. This loading rate dependence is consistent with that observed from as-received TP316L SS and is typical characteristics of austenitic SS. Thus it is indicated that the loading rate dependence of TP316 L SS is not altered by cold-work, even though its fracture resistance is considerable reduced. Also, it is expected from this result that the dynamic loading effect on fracture resistance of irradiated TP316L SS can be ignored.

Figure 8 presents the cyclic *J-R* curves of as-received and cold-worked TP316L SSs at 316°C, together with corresponding monotonic *J-R* curves. In Fig. 8(a), the cyclic *J-R* curves of as-received TP316L SS are much lower than corresponding monotonic *J-R* curves; i.e., the cyclic load considerably reduces fracture toughness of as-received TP316L SS. According to the previous studies, fully reversed cyclic load significantly reduces fracture resistance of materials, and the reduction is associated with crack-tip sharpening developed during the compressive step of cyclic loading (Chowdhury et al.(2015), USNRC (1996), Kim et al. (2016)). As shown in Fig. 8(b), however, the cyclic *J-R* curves of cold-worked TP316L SS simulating irradiation embrittlement are nearly identical to corresponding monotonic *J-R* curves; i.e., the cyclic loading effect on fracture resistance is insignificant for cold-worked TP316L SS. This is because the fracture resistance of cold-worked TP316L SS is low enough so that the crack sharpening effect induced by cyclic load is relatively insignificant. Also, it is believed that the cyclic loading effect on the fracture resistance of irradiated TP316L SS might be insignificant.

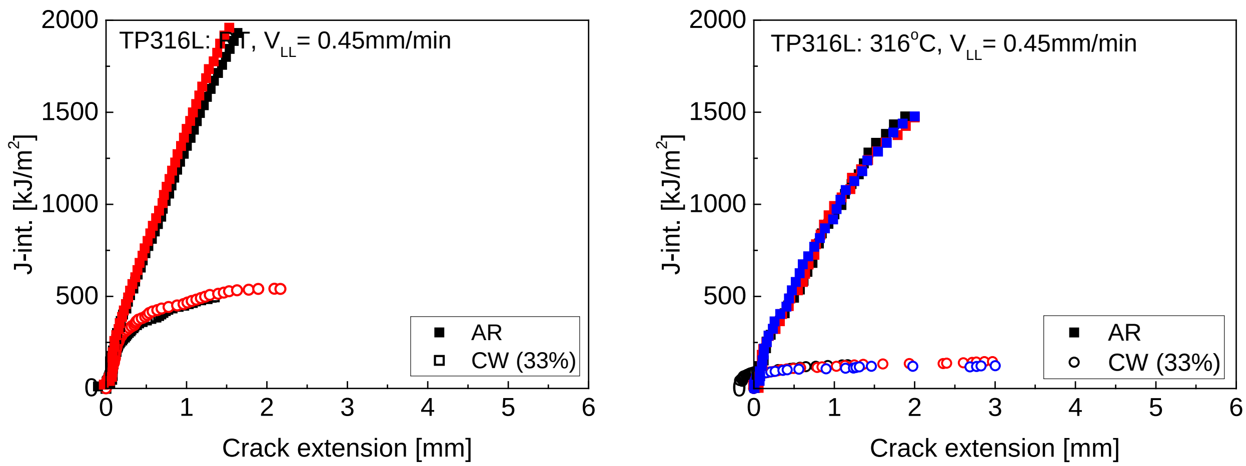

(a) RT (b) 316°C

Fig. 6 Comparison of *J-R* curves of as-received and cold-worked TP316L SSs

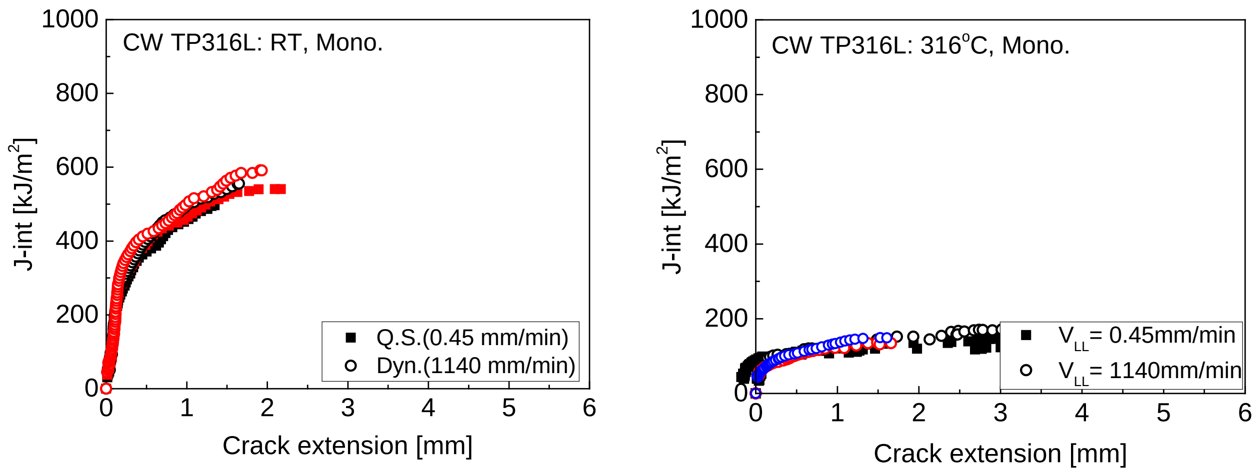

(a) RT (b) 316°C

Fig. 7 Comparison of quasi-static and dynamic *J-R* curves of cold-worked TP316L SSs

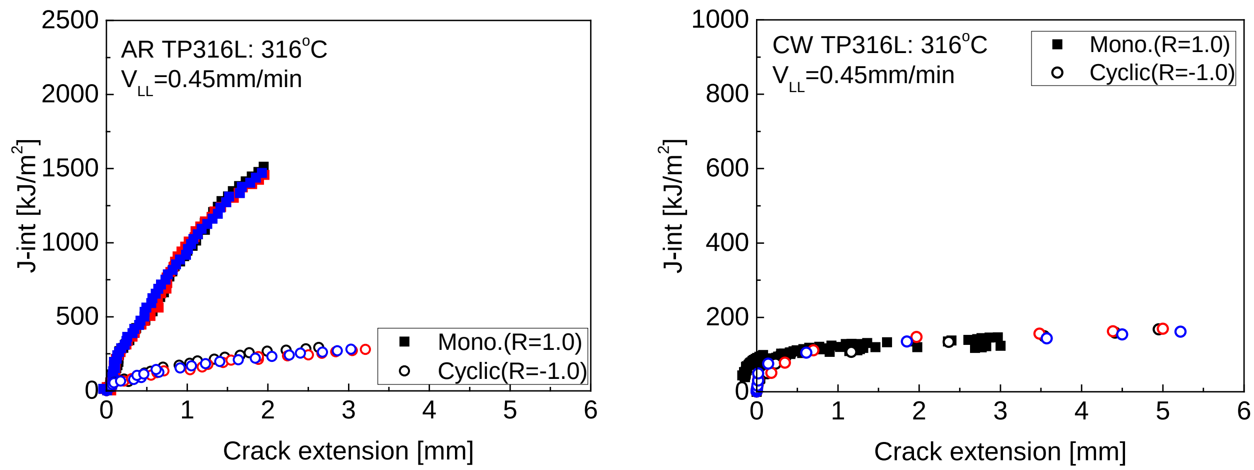

(a) RT (b) 316°C

Fig. 8 Comparison of monotonic and cyclic *J-R* curves of as-received and cold-worked TP316L SSs

CONCLUSION

This study conducted *J-R* fracture toughness test on cold-worked stainless steel (SS) under dynamic and cyclic loading conditions to investigate the effect of seismic loading on the fracture behaviour of irradiated austenitic SSs. Also, tensile tests were conducted under quasi-static and dynamic displacement rates. From the results the following conclusions were drawn:

1) Cold-work of TP316L SS properly simulated the hardening and embrittlement of TP316L SS by irradiation.
2) Dynamic loading effects on the deformation and fracture resistance of cold-worked TP316L SS simulating irradiation embrittlement were negligible at both RT and 316°C. This is the same as that observed from as-received TP316L SS.
3) Cyclic loading considerably reduced the fracture resistance of as-received TP316L SS, but the reduction by cyclic load was less significant for cold-worked TP316L SS compared to as-received TP316L SS. In particular, the cyclic loading effect was almost negligible at 316°C.

REFERENCES

Saji, G. (2014). "Safety goals for seismic and tsunami risks: Lessons learned from the Fukushima Daiichi disaster," *Nuclear Engineering & Design*, 280 449–463.

Stevenson, J.D. (2014). "Summary of the historical development of seismic design of nuclear power plants in Japan and the U.S.", *Nuclear Engineering & Design*, 269 160–164.

Nakamura, I. and Kasahara, N. (2015). "Excitation tests on elbow pipe specimens to investigate failure behavior under excessive seismic loads," *Proceeding of PVP2015*, PVP2015-45711.

Paul, S.K., Sivaprasad, S., Dhar, S., and Tarafder, S. (2011). "Key issues in cyclic plastic deformation: Experimentation," *Mechanics of Material*, 43 705–720.

Goyal, S., Gupta, S.K., Sivaprasad, S., Tarafder, S., Bhasin, V., and Vaze, K.K. (2013). "Low cycle fatigue and cyclic plasticity behavor of Indian PHWR/AHWR primary piping material," *Procedia Engineering*, 55 136-143.

Singh, P.K., Ranganath, V.R., Tarafder, S., Prasad, P., Bhasin, V., Vaze, K.K. and Kushwaha, H.S. (2003). "Effect of cyclic loading on elastic-plastic fracture resistance of PHT system piping material of PHWR," *Int. J. Pressure Vesssels and Piping*, 80, 745–752.

Chowdhury, T., Sivaprasad, S., Bar, H.N., Tarafder, S. and Bandyopadhyay, N.R. (2015). "Cyclic fracture behaviour of 20MnMoNi55 steel at room and elevated temperatures," *Fatigue & Fracture Engineering Materials Structure*, 38, 813–827.

Roy, H., Sivaprasad, S., Tarafder, S. and Ray, K.K. (2009). "Monotonic vis-à-vis cyclic fracture behaviour of ANSI 304LN stainless steel," *Engneering Fracture Mechanics*, 76, 1822–1832.

USNRC. (1996). The Effect of Cyclic and Dynamic Loading on the Fracture Resistance of Nuclear Piping Steels, *NUREG/CR–6440*.

Kim, J.W., Choi, M.R., and Kim, Y.J. (2016). "Effect of loading rate on the fracture behavior of nuclear piping materials under cyclic loading conditions," *Nuclear Engneering & Technology*, 48, 1376–1386.

Shah, V.N. and Macdonald, P.E. (1993). Aging and Life Extension of Major Light Water Reactor Components, Elsevier Science Pub., Amsterdam.

Delliou, P.L. and Saillet, S. (2015). "Integrity and life assessment of cast duplex stainless steel elbows and EdF PWR main collant piping," *Proceeding of PVP2015*, PVP2015-45231

Jitsukawa, S., Shiba, K., Hishinuma, A., Alexander, D.J. (1996), "Comparison of elastic-plastic fracture toughness of irradiated and cold-worked JPCA using miniaturied DCT specimens," *J. of Nuclear Materials*, 233-237 152-155.

Pawel J.E., Rowcliffe, A.F., Lucas, G.E., Zinkle, S.J. (1996). "Irradiation performance of stainless steels for ITER application," *J. of Nuclear Materials*, 239 126-131.

ASTM (2015). "Standard test method for measurement of fracture toughness," ASTM E1820-15.

ASTM (2009). "Standard test method for tension testing of metallic materials," ASTM E8/E8M-09.

Kim, J.W., Byun, T.S. (2010), "Analysis of tensile deformation and failure in austenitic stainless steels: Part II – Irradiation dose dependence," *J. of Nuclear Materials*, 396 10-19 .